Increased kilo-electron-volt x-ray yields from Z-pinch plasmas by mixing elements of similar atomic numbers

C. Deeney,* P. D. LePell, B. H. Failor, and S. L. Wong
Physics International Company, 2700 Merced Street, San Leandro, California 94577

J. P. Apruzese, K. G. Whitney, J. W. Thornhill, and J. Davis
Naval Research Laboratory, 4555 Overlook Avenue SW, Washington, DC 20375

E. Yadlowsky, R. C. Hazelton, and J. J. Moschella
HYTECH Research Corporation, 104 Center Court, Radford, Virginia 24141

T. Nash
Sandia National Laboratories, 1515 Eubank Avenue, Albuquerque, New Mexico 87185

N. Loter
Maxwell Laboratories, Inc., 8888 Balboa Avenue, San Diego, California 92123
(Received 4 November 1994)

Magnesium-coated aluminum wire array Z pinch plasmas have been tested on a 4-MA, 6-TW pulsed electrical generator. A mixture of 80% aluminum and 20% magnesium is observed to maximize the radiated kilovolt x-ray yield at ≥ 50 kJ, which is 50% higher than that obtained with pure aluminum. Spectroscopic analysis and collisional radiative equilbrium models with radiation transport are employed to show that the aluminum-magnesium mixture reduces the opacity of the strongest emission lines, thus increasing the yield by increasing the probability of photon escape. Furthermore, the spectroscopic data also point to the presence of a strong temperature gradient in the pinched plasma that results in the outer magnesium coating of the wires having a higher electron temperature in the pinch. This temperature difference also plays a role in enhancing the kilovolt x-ray yield. The observation of a higher magnesium electron temperature offers evidence that the magnesium reaches the axis first, forming a core that is compressed and heated by the imploding mass of aluminum. Since the emissions from the core are not absorbed by the outer aluminum, the yields are increased. By comparison, aluminum-magnesium alloys imploded on a different but similar generator do not show a temperature difference.

PACS number(s): 52.25.Nr, 52.65.−y, 52.55.Ez, 52.50.Lp

I. INTRODUCTION

Since the invention of imploding wire array Z-pinch plasmas [1–4] in the late 1970s, numerous researchers have been involved in scaling these plasma x-ray sources to high current generators such as Double-EAGLE, Blackjack-5, and SATURN. These generators can implode large enough masses (>100 μg/cm) that for low atomic number elements ($1<Z<13$), the principal resonance lines of the K shell are optically thick. Recent theoretical studies [5] of the scaling of K-shell emissions to higher currents have indicated that both the opacity and the mass of the plasma play a major role in determining the scaling regime, that is, if the yield scales as the mass squared or as the mass. To increase the emissions from high current Z pinch plasmas, therefore, it would be beneficial to decrease the opacity of the major resonance lines. Mixing two elements, for instance, would double the number of lines emitted while reducing their opacity for the same mass load.

Apruzese and Davis [6] quantified the amount by which the mixing of elements of similar atomic number (near Z) could increase the radiated power from an optically thick plasma of a given mass. In particular, Fig. 1 of that paper indicated that for an approximately 50%:50% mix of sodium and neon ions, the radiated power from the Z-pinch plasma would double (compared to pure Ne) if it were optically thick, whereas it would remain almost unchanged for an optically thin plasma. This paper investigates this effect experimentally. Since there is no convenient way to mix sodium and neon, we selected composite aluminum and magnesium wire arrays for our experiments.

We show curves of the predicted power from an optically thin and an optically thick plasma with various aluminum and magnesium mixtures in Fig. 1. These powers were calculated using a collisional radiative equilibrium (CRE) model [7] with full radiation transport for an electron temperature of 300 eV. The optically thick case represents a plasma that is consistent with a Z-pinch generated by a 4-MA current source ($n_e=10^{21}$ cm^{-3}) and a 3 mm diameter (typically 290 μg/cm). The optically thin case has the same parameters, but with absorption switched off. At 300–600 eV, the temperature is a little below optimum for the aluminum; hence the power increases linearly with the magnesium fraction in the opti-

*Present address: Sandia National Laboratories, MS-1194, 1515 Eubank Avenue, Albuquerque, NM 87185.

cally thin case. For both temperatures, the optically thick power maximizes for a mix rather than pure Al or Mg. This represents the effect of line opacity reduction folded in with each element's radiating efficiency at the given temperature. The opacities can be substantial: for pure Mg, the He-α line has an optical depth of 562 at 300 eV and 36 at 600 eV. The corresponding depths for the Al He-α line at the two temperatures are 1757 and 191, respectively. At 600 eV, line photon reabsorption in the thick case results in ladder ionization and additional overstripping of the Mg, rendering it a less effective radiator than Al. A fuller picture of the radiation physics of the near-Z power increase comes from considering two types of photon escape probability.

Following the creation of a line photon by collisional excitation (mostly) or recombination to the upper bound level of the transition, there is a chance that the photon will escape the plasma without further interaction. This is described by the single flight escape probability P_e. For the most copiously radiating optically thick lines, however, the photon is usually absorbed and reemitted a number of times before either escaping or being collisionally quenched in the plasma. The probability that the photon ultimately escapes after a number of such interactions is P_u. Figure 2(a) schematizes the difference between these escape probabilities. A fuller discussion along with analytic approximations appears in Ref. [6]. For the present application, P_u is the most relevant quantity. Specific numerical results of these quantities are presented in Fig. 2(b) for the He-α line from an Al plasma at 300 eV and Mg at 600 eV, with parameters similar to those attained in the experiments described below.

The extent of enhancement of line emission depends upon the quantitative functional form of P_u vs the element fraction. Referring to Fig. 2(b) and the dotted P_u curve for Al, reducing the element fraction from 1.0 to 0.8 increases P_u from 0.087 to 0.097 or 11.5%. Therefore, since the number of created Al photons drops by 20% but the fraction of these escaping increases by 11.5%, removing 20% of the Al reduces the He-α line output by only 11%. However, the removed 20% of Al can be replaced by, for instance, Mg, whose P_u at an element fraction of 20% is 0.64 for these conditions. Therefore, the added increment of Mg will be a much more efficient He-α radiator than the removed, nearly saturated Al. This is how the mixing of elements can enhance line emission. If the elements separate and the Mg turns out to be hotter that the bulk of the Al, the effect can be accentuated.

For our experiments, we had to use a coating technique to deposit magnesium onto aluminum wires since fine magnesium wires are difficult to make and aluminum-magnesium alloys contain only up to 5% Mg. The exact details of this coating technique will be described in Sec. II.

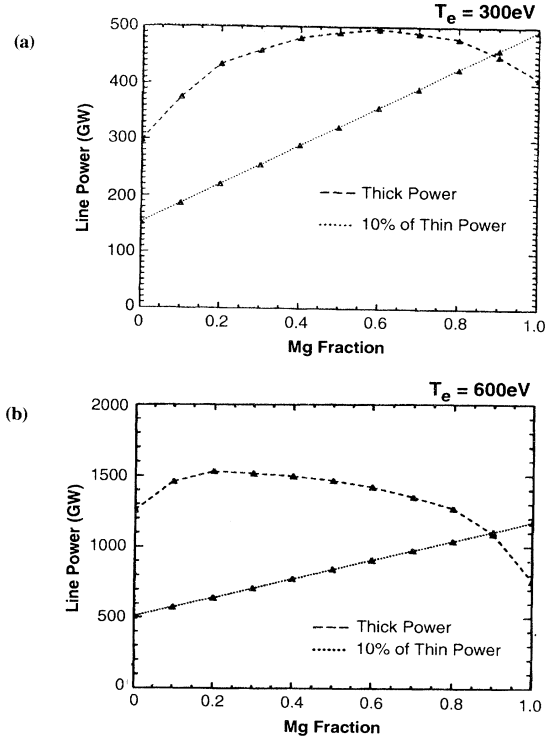

FIG. 1. Predicted kilovolt K-shell x-ray output from a 3-mm-diam plasma with an aluminum-magnesium mixture for both an optically thick and an optically thin plasma (dotted curve): the plasma electron temperature is (a) 300 eV and (b) 600 eV. For the optically thick case, a mix optimizes the radiated power.

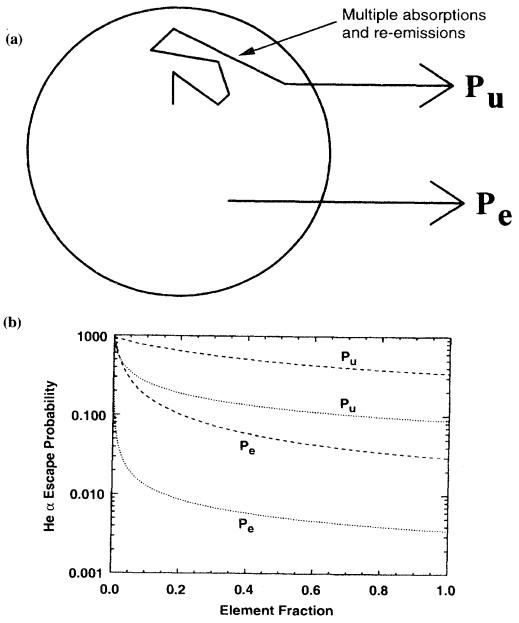

FIG. 2. (a) Two different escape probabilities for a photon from a plasma: the ultimate escape probability P_u and the local single flight escape probability P_e. P_u depends on P_e and on the probability of collisional loss P_q. (b) As the element fraction increases, both probabilities of escape decrease. The optimum is a mix that will maximize the combined probability of escape. This result is for aluminum (dotted lines) and magnesium (dashed lines). The plasma diameter is 3 mm and the electron density is 10^{21} cm^{-3}. The line modeled is He-like $1s^2$-$1s2p\ ^1P_1$.

In Sec. II we will describe the Double-EAGLE generator and our wire array hardware, including the coating technique. Our extensive range of x-ray diagnostics are also described in that section.

In Sec. III we present our experimental results, including a demonstration of the yield enhancement. The x-ray data presented will show evidence for temperature gradients in the pinch and we will describe this spectroscopic analysis. These temperature gradients have an important implication for our interpretation of the results, which are discussed in Sec. IV, although we will show that opacity reduction is still a contributing effect. In conclusion, we will discuss the implications of these results for future experiments and load designs in Sec. V.

II. HARDWARE CONFIGURATION FOR THE COATED WIRE EXPERIMENT

The Double-EAGLE generator [8] at Physics International is a 4-MA, 6-TW waterline pulsed power machine. A central vacuum load region is fed through an insulator stack by two triplate modules. Each module is composed of a 3.5-MV Marx bank (500 kJ each), a gas-switched water transfer capacitor, a charged pulsed line and a pulse forming line (both with self-break water switches), a transformer section, and finally a vacuum diode.

A single magnetically insulated post hole convolute combines the current in vacuum from the triplate feed into a wire array load as shown in Fig. 3. A typical load current pulse and kilovolt x-ray pulse are shown in Fig. 4. As can be seen from Fig. 4, for a nominal 60-kV charge on each Marx capacitor, we get a 3.5–3.8-MA peak current into the imploding load: the time to peak current into a short is 110 ns. The load current is measured by a self-integrating Rogowski coil, which is calibrated with a small pulser and then verified using short circuit tests on Double -EAGLE.

On a typical shot, we field an extensive array of x-ray diagnostics as shown in Fig. 5 and described in Ref. [9]. A gated time-resolved microchannel plate (MCP) pinhole camera, gated by 5 ns, −1-kV pulses, monitors the dynamics of the pinched plasma. Another gated microchannel plate camera is attached to a 5-cm-radius-of-curvature MICA crystal ($2d = 9.942$ Å) spectrometer to measure the K-shell lines from magnesium and aluminum.

The kilovolt x-ray pulsewidth, power, and yields are measured with 4-μm-thick kimfol, 8.4-μm-thick kapton filtered x-ray diodes, and 4-μm-thick kimfol and 8.4-μm-

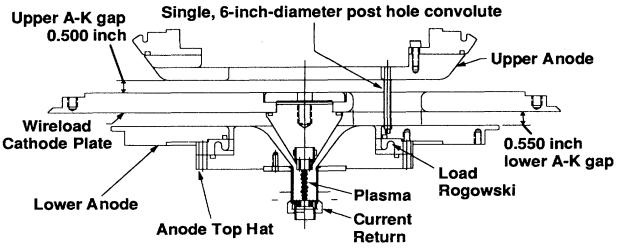

FIG. 3. Double-EAGLE post hole convolute and wire array hardware. A-K refers to the anode cathode.

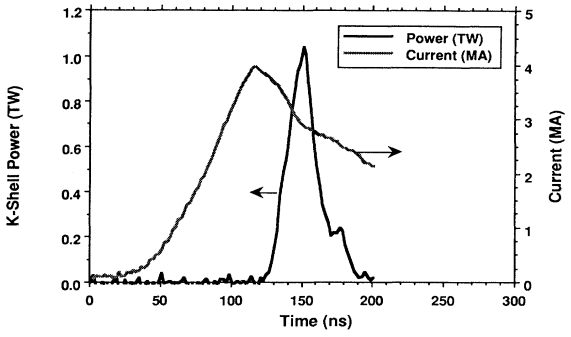

FIG. 4. Measured load current and total kilovolt x-ray power pulse for a 80%:20% Al-Mg wire array.

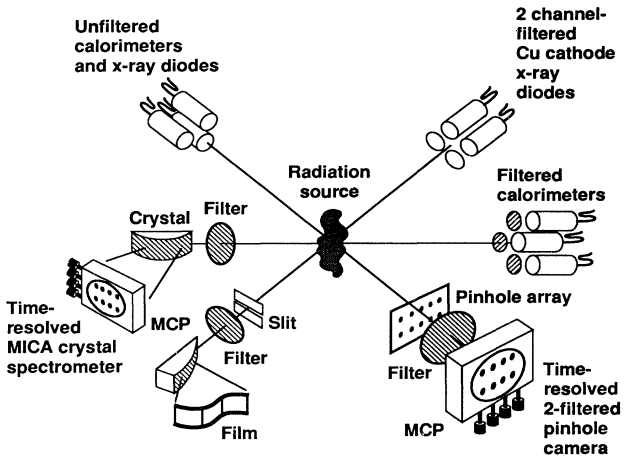

FIG. 5. Double-EAGLE diagnostic arrangement.

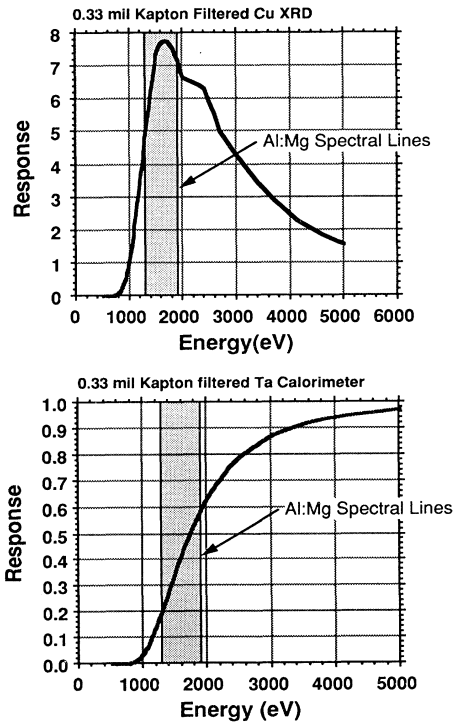

FIG. 6. Relative detector responses versus photon energy for our filtered copper XRDs and tantalum calorimeters.

thick kapton filtered calorimeters. We use an unfiltered copper x-ray diode to measure the total (extreme ultraviolet plus kilovolt) radiation. Figure 6 shows the filtered detection responses.

The time-integrated but axially resolved (1-mm resolution) spectrum is recorded with an ARACOR HW-1000 spectrometer. The recording medium is Direct Exposure Film (DEF-392) and the crystal is a 5-cm-radius-of-curvature MICA crystal.

Our standard wire array hardware consists of two graphite electrodes with 12 wires strung between them. This assembly plugs into the cathode and anode hardware. To make these wires, LeBow Company mounted fifty 10-cm-long aluminum wires into a fixture that was rotated above a magnesium evaporation unit to produce a uniform deposition at about 30 Å/min. The deposition thickness was verified by using a microbalance. These wires were then mounted into our standard array mount, which sets the wire array length at 2 cm.

For this experiment we chose to use a 15-mm-diam load hardware, since previous radius scaling experiments with pure aluminum showed that this was near optimum [3]. Double-EAGLE was operated at a higher charge voltage than that used in the previous aluminum experiment (Ref. [3]), so we increased the average mass loading to 290 μg/cm. Due to a limited availability of aluminum wire thicknesses, we had a range of actual mass loadings for the different mixes as shown in Table I. In Table I, we tabulate, by aluminum percentage, the Al:Mg mixture's mass loadings, aluminum wire diameters, magnesium coating thicknesses, and the number of wires used in these experiments.

III. MEASUREMENT OF ALUMINUM AND MAGNESIUM *K*-SHELL X RAYS

A. Kilovolt x-ray yield results

For the shot matrix listed in Table I, we determined that the 80%:20% mix produced the maximum yield, as shown in Fig. 7(a). The mixtures definitely produced more yield than an equal mass, pure aluminum pinch, more even than the best aluminum performance [3]. For completeness, we have summarized all the data in Table II and have marked the shot numbers on the individual data points. Two subsequent shots (3074 and 3080) are shown at the 80%:20% mix. Since the variation in mass loading translates to a variation in implosion time (hence kinetic energy), we decided to also normalize these yields to the kinetic energy. To normalize the yield data, therefore, we employed a zero-dimensional implosion code. It incorporates the Double-EAGLE electrical circuit to calculate the kinetic energy in each case using the model discussed in Ref. [10]. Our calculations used the measured pinched plasma size as the final diameter to stop the zero-dimensional calculations. In Fig. 7(b) we plot the yield divided by the calculated kinetic energy. Again, this confirms that the 80%:20% Al:Mg mix produced the highest efficiency with an average of 130% or a kinetic energy conversion factor of 130%. Previous work has shown that the measured *K*-shell x-ray yields can exceed those predicted assuming only kinetic energy input [3,11]. The fact that the measured kilovolt yields exceed the input kinetic energy with these mixtures is further evidence that there are other energy input mechanisms.

TABLE I. Summary of the coated wire array loads. All loads were 15 mm in diameter and 2 cm long. Double-EAGLE was operating at a 60-kV Marx charge.

Al:Mg mix (%:%)	Aluminum wire thickness (μm)	Magnesium coating thickness (μm)	Number of wires	Mass loading (μg/cm)
100:0	30.5		14	276
90:10	30.5	1.25	12	262
80:20	30.5	2.75	12	295
70:30	30.5	4.25	12	337
50:50	20.3	5.85	16	280
40:60	20.3	8.35	12	262
30:70	20.3	11.35	12	245

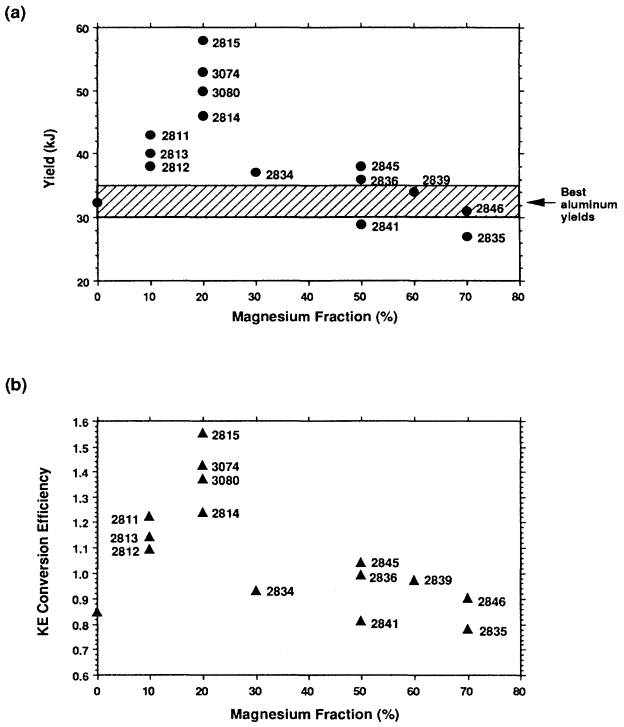

FIG. 7. Measured kilovolt x-ray yield from the wire arrays described in Table I. The (a) measured yields are also normalized to the implosion kinetic energy in (b).

Using a CRE analysis allows us to directly calculate the radiated powers (as presented in Fig. 1), so for completeness we show the experimentally measured radiated peak powers in Fig. 8. The measured powers do show a trend similar to the yields. There was a significant variation, however, in the x-ray yields and powers that we measure: more so than with standard aluminum loads. In particular, the shots taken later in the sequence tended to show lower yields. For example, shot 2834 was made much later in the sequence than shot 2815. This degrading, we believe, was due to oxidation of the magnesium

TABLE II. Summary of the experimental results for the aluminum-magnesium wire array implosions. FWHM denotes full width at half maximum.

Shot	Magnesium fraction (%)	Mass loading (μg/cm)	Implosion time (ns)	Yield (kJ)	Kinetic energy conversion efficiency (%)	x-ray pulse FWHM (ns)	Kilovolt x-ray power (GW/cm)
2811	10	262	75	43	122	28	527
2812	10	262	95	38	109	33	516
2813	10	262	92	40	114	27	633
2814	20	295	93	46	124	35	571
2815	20	295	87	58	155	25	1028
2834	30	337		37	93	41	529
2836	50	280		36	99	16	888
2841	50	280	100	29	81	31	562
2845	50	280	93	38	104	22	635
2839	60	262	87	34	97	25	625
2835	70	245		27	78	35	360
2846	70	245	90	31	90	22	503

coating on the wires. Micrographs of the wires some weeks after the tests indicated bubbling of the magnesium coating. If the magnesium oxidized and bubbled, this could explain the variability in implosion time and radiation performance. Future experiments will use a storage container filled with inert gas to prevent oxidation of the coating.

Notice that there is one important difference between the results in Figs. 7 and 8 and those in Fig. 1. Theoretically, a mixture of Mg and Al should have a broad peak of enhanced yields with a peak somewhere between 20% and 50% Mg. Experimentally, the peak was observed to be located at 80% Al and 20% Mg. In an attempt to explain this behavior, we have analyzed our spectroscopic data.

B. Aluminum-magnesium *K*-shell spectra

Figure 9 shows three examples of the time-integrated aluminum-magnesium spectra recorded by the Aracor instrument. We have corrected the measured spectral for crystal, film, and filter responses. These spectra are for (a) shot 2814 (80%:20% mix), (b) shot 2845 (50%:50% mix), and (c) shot 2839 (60%:40% mix). We can make a few straightforward observations from these time-integrated spectra: (i) the ratio of the magnesium Ly-α to the He-α line is larger than the ratio for aluminum Ly-α to the He-α line, (ii) the β lines are very weak in most cases, and (ii) the fraction of the energy radiated in the magnesium *K*-shell lines is large for even a small magnesium fraction (see Fig. 10).

The Ly-α to He-α line ratio is a good measurement of electron temperature even in optically thick plasmas, provided a self-consistent CRE model with radiation transport is used to analyze the data [7]. The procedure

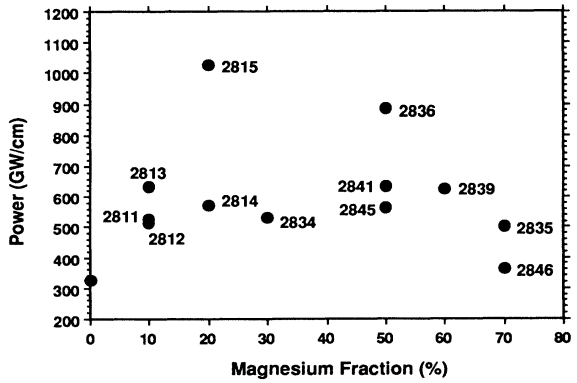

FIG. 8. Measured total kilovolt x-ray powers versus magnesium fraction.

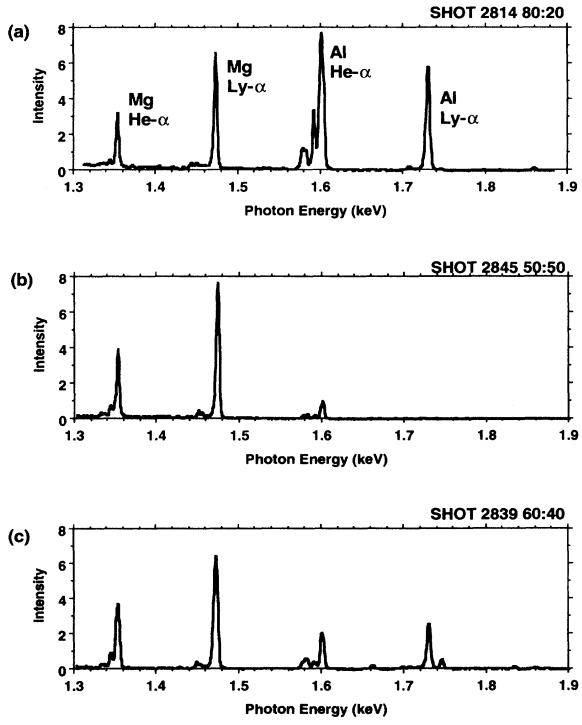

FIG. 9. Time-integrated *K*-shell spectra for three different mixtures: (a) 80%:20%, (b) 50%:50%, and (c) 60%:40%.

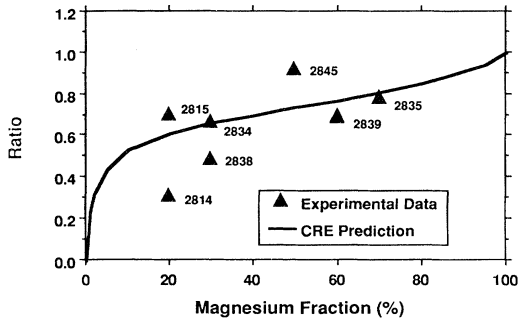

FIG. 10. Measured ratio of the magnesium line energy to the total line energy versus magnesium fraction.

for diagnosing the temperature and the density is described in detail in Ref. [7]. Briefly, for a given measured pinch diameter, the Ly-α to He-α ratio is calculated for hundreds of combinations of temperature and density, and isocontours of the ratios are plotted based upon this calculated data, as a function of temperature and density. If the vertical axis is temperature and the horizontal axis represents density, these line ratio contours are found to be mostly parallel to the horizontal axis, since the ratio is principally a function of temperature. A similar plot is constructed for the He-α line power. In the temperature regime of interest, the He-α power is mostly sensitive to density, since increasing the temperature shifts the line radiation to the H-like stage rather than enhancing He-like lines. Therefore, the He-α power contours are mostly parallel to the vertical axis. For a given shot, the line ratio and the He-α power are measured. The intersection in temperature-density space of the horizontal contour representing the line ratio and the vertical contour equaling the measured power defines a unique diagnosed ion density and electron temperature.

For our analysis, we used time-integrated spectra like those shown in Fig. 9. The plasma diameter is determined from the time-resolved pinhole images as shown in Fig. 11. The time-resolved images are 5 ns in duration and they are synchronized with the radiation power pulse. The images in Fig. 11 show the pinch at the time of maximum power and then the growth of instabilities at late time. For most of our shots, the plasma diameters at the time of peak power were in the range of 2.5–3.0 mm [see Fig. 11(c)].

We have determined electron temperatures and ion densities for the full range of Al:Mg mixtures (shown in Fig. 12). The data show consistently that the magnesium temperature is hotter ($\sim$600 eV) than that of the aluminum ($\sim$300 eV), i.e., the bulk of the magnesium and the aluminum plasmas are spatially separate. Another indication that the plasmas are spatially separate comes from the inferred ion densities. Namely, the ion densities are in some cases higher than they would be if all the initial load mass were uniformly distributed (around 10^{20} cm^{-3}). The spatial separation of the aluminum and the magnesium depends on the way in which the wires explode and then implode, as discussed in Sec. IV. Most of the calculations were performed assuming a 3 mm diameter for both the Al and Mg regions. However, calculations done for other assumed diameters show that the conclusion of different temperatures for the two elements is unaffected.

The second observation from the spectra was that the β lines were weaker than the CRE predictions. This was consistently the case through all the data. Only when the background fog level on the DEF-392 film was low (<0.3) did we detect the magnesium Ly-β line, for example, in shot 2839. Typically, CRE predictions for aluminum or magnesium plasmas at our density and temperature conditions would show β lines that were one-quarter or so of the α lines. We are trying to resolve this discrepancy. It appears to be correlated with the observation that the α lines are broadened more than the static CRE calculations assume. For example, the ions in a Z-pinch plasma are predicted to have higher temperatures than the electrons for a large fraction of the pinch duration [12] and therefore there will be more Doppler broadening than a static CRE model calculation predicts.

In Fig. 10 we illustrate that the fraction of the energy radiated in the magnesium lines increases much faster than the percentage of magnesium. This is to be expected since at small fractions the magnesium will be relatively optically thin so the radiation rates will increase as the density squared until opacity starts to limit the emissions and the rate of increase falls off. These trends are seen in Fig. 10 and the data agree well with a CRE prediction based on a two-temperature model for the magnesium and aluminum. We will discuss these calculations in more detail in the following section.

IV. DISCUSSION

A. Near-Z opacity effects

Due to this observation of the different temperatures of the two elements, we first have to evaluate the increase in x rays as a function of the Mg fraction to determine how opacity is affecting the yields. In Fig. 13 we plot the predicted K-shell powers with and without opacity for aluminum-magnesium mixtures where the magnesium is assumed to be at 600 eV and the aluminum is at 300 eV. At these temperatures, the magnesium is at near optimum temperature whereas the aluminum is slightly too cold for efficient K-shell production. Figure 13 shows that as a result of these temperature differences, a small amount of magnesium admixture causes a rapid increase in the radiated power when opacity is included. Clearly the opacity still plays a role since the slope of the power curve is initially greater than that of an optically thin (dotted curve) case. However, as the magnesium fraction is increased, the kilovolt x-ray power is almost constant, unlike the single temperature cases presented in Fig. 1. For a single temperature, the near-Z elements are roughly comparable in their ability to radiate, so as the pinch tends to a single material, the opacity limits the radiation to less than that for a 50%:50% mix. In the calculations depicted in Fig. 13, because the magnesium is a better radiator at its higher, 600-eV electron temperature, the radiated power from a pure magnesium pinch would exceed that of a pure 300-eV aluminum plasma. The rap-

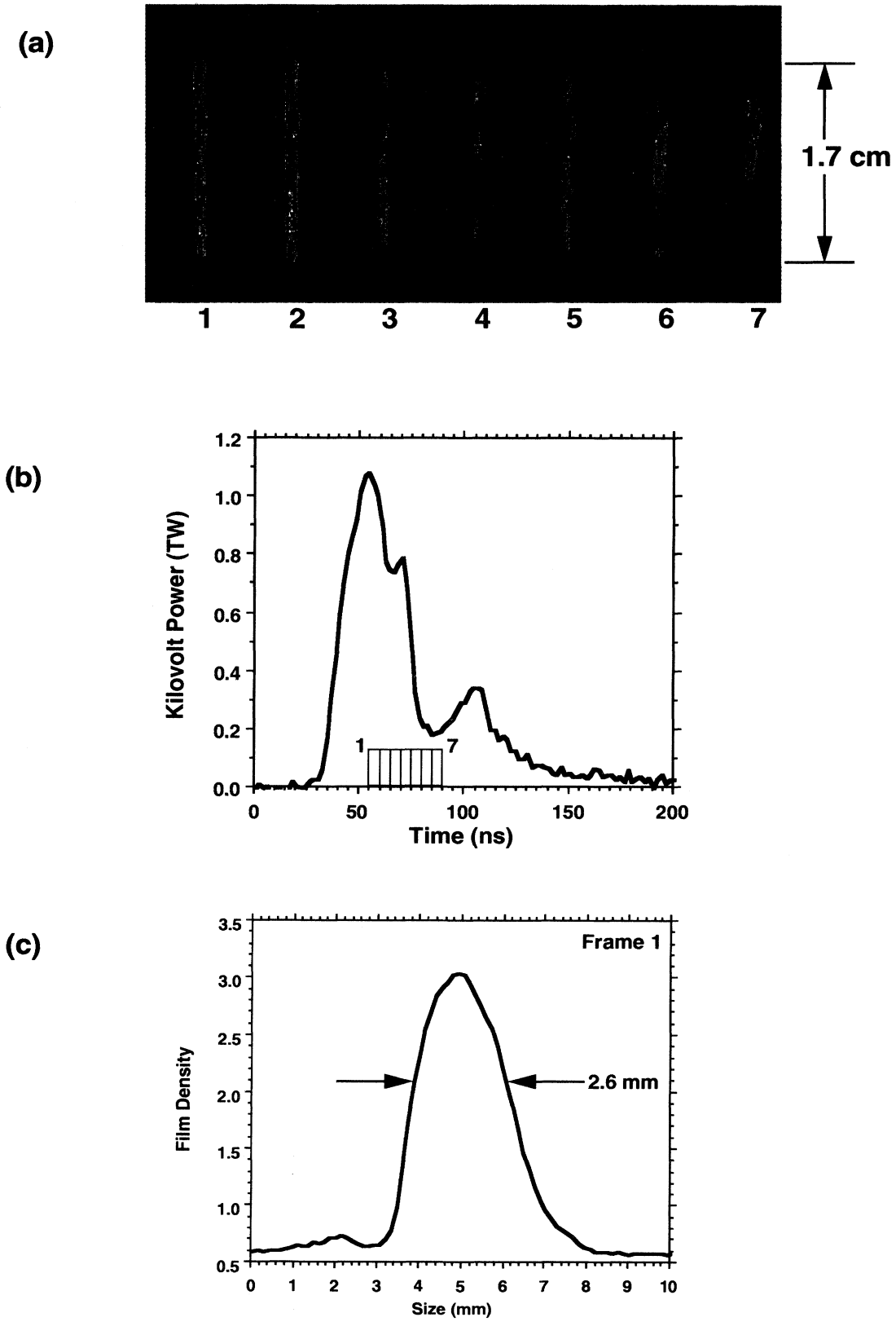

FIG. 11. Kilovolt time-resolved x-ray images of an 80%:20% implosion (shot 2814). In (a) we show the actual images in false color. The relationship of these images to the kilovolt power pulse are shown in (b) and an axially integrated, radial line out is shown in (c). Note that only a 1.7 cm length is observed due to the 22° viewing angle and the hardware geometry.

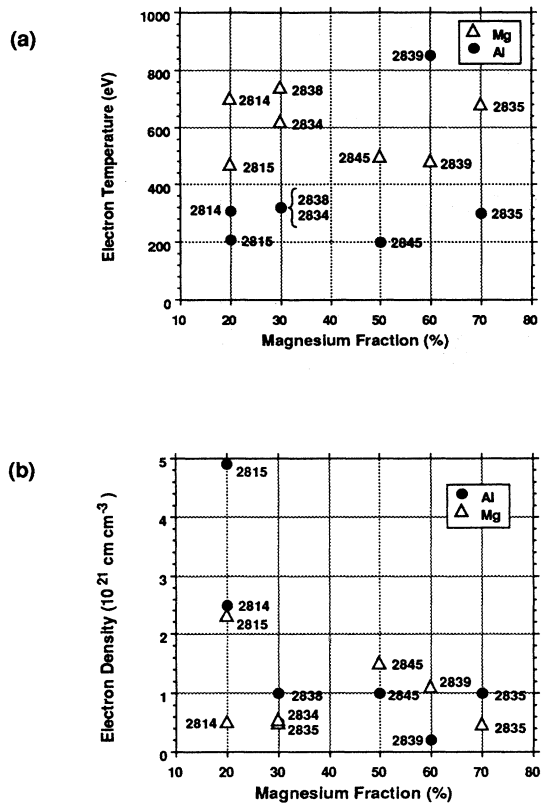

FIG. 12. Measured (a) electron temperature and (b) electron density from all the aluminum-magnesium wire arrays. Notice that the electron temperatures deduced from the magnesium lines are higher than those inferred from the aluminum lines, although the electron densities are generally lower. This is an indication that the plasmas are not uniformly mixed.

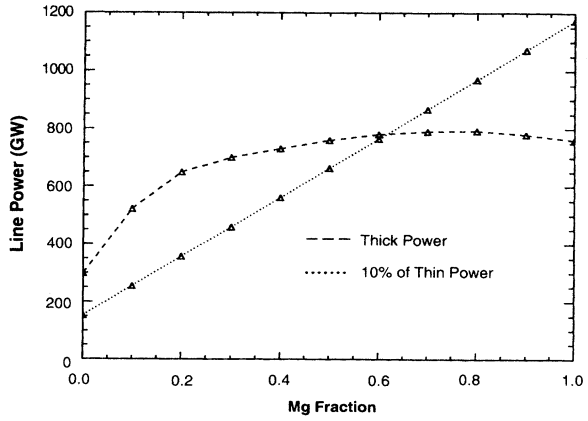

FIG. 13. Predicted kilovolt K-shell x-ray power from an aluminum-magnesium mix with the same conditions as in Fig. 1, but with the aluminum having an electron temperature of 300 eV and the magnesium having an electron temperature of 600 eV. The hotter magnesium changes the behavior of the CRE predictions, but the mix still produces more yield than pure pinches. This trend better matches the observed powers in Fig. 8.

id increase in the fraction of the total energy radiated in the magnesium lines observed in Fig. 10 is also consistent with this observation. The CRE model curve shown in Fig. 10 used the two measured temperatures.

This illustrates a subtle opacity effect. If there is a part of the pinched plasma at a higher temperature, then by mixing in a near-Z element that will both preferentially get into that region and also be relatively optically thin, the radiation rates can be increased significantly since the photons coming from the hot region will not be absorbed by the cold outer material. This obviously depends on the exact geometry of the pinched plasma, which we will discuss in Sec. IV C.

B. Spectroscopic analysis of temperature gradients in coated wire array Z pinch plasmas

As discussed above, the bulk of magnesium and aluminum exist in different regions with different densities as well as temperatures. Unfortunately, without more detailed space- and time-resolved spectra, we cannot definitively speculate on the ion distribution in the pinch, but we can try to assess it by fitting a multizone CRE analysis to our data. For this comparison, we selected shot 2814. Once we have studied these coated loads with improved time- and space-resolved spectrometers, we will be able to perform a more thorough analysis.

Table III lists the zone sizes, composition, temperatures, and densities for a CRE calculation that produces a spectrum (Fig. 14) that matches the He-α power and the Ly-α to He-α ratio for both aluminum and magnesium in shot 2814. In this calculation, all of the magnesium and 90% of the aluminum radiates in the K shell. This suggests that only a small hot core of magnesium surrounded by a smaller volume of cooler aluminum is needed to match the spectra.

Now, it is unlikely that the plasma has two or three sharply defined zones. Rather, there is probably a very steep temperature gradient and the measured temperature is averaged over some fraction of the pinch. An obvious test of our deduction that coated arrays have a large temperature gradient as well as spatial separation between Al and Mg ions would be to look at data from an aluminum-magnesium alloy shot. Since there is no initial spatial separation between ions in an alloy, similar temperatures should be calculated on axis from the Al and the Mg spectra. Such data were obtained at Maxwell Laboratories from wire array implosions on their Blackjack-5 generator. Blackjack-5 is very similar to Double-EAGLE in load current. In experiments, using aluminum 5056, which has a 5% magnesium content, the spectrum shown in Fig. 15 was produced. In this case, a CRE analysis of the magnesium and the aluminum lines does yield similar temperatures as expected, 300 eV for Mg and 350 eV for Al. Note that this small discrepancy may be due, in part, to steep temperature gradients in the alloy plasma, which we are unable to discern by this analysis procedure.

TABLE III. Using a three-zone CRE model, with the above parameters, the He-α and the Ly-α lines for Al:Ma shot 2814 can be matched with a predicted spectrum (in Fig. 14).

Zone	Radial extent (cm)	Element(s)	Ion density (cm^{-3})	Temperature (eV)
1	0.00–0.05	Mg	1.8×10^{20}	680
2	0.05–0.06	Al	1.4×10^{21}	310
3	0.06–0.15	Mg plus Al	$\sim2\times10^{18}$	310

C. Wire array dynamics

The question is, How does this temperature gradient come about? It is well known that one-dimensional simulations show hot cores in the pinch [13]. These calculations generally show that there is a low density plasma present in the core just prior to stagnation. Part of this interior plasma is placed in calculations intentionally to provide numerical stability and some of it is plasma that is pushed into the interior regions by shocks and by the $\mathbf{J}\times\mathbf{B}$ forces generated by the current and the magnetic fields that have diffused into the interior of the pinch once it assembles into a cylinder. Since a low density plasma is not an effective radiator, its stagnation state is characterized by strong shock behavior whereby low compressions and large temperature are achieved. Radial temperature and density profiles are shown in Fig. 16 for a 300-μg/cm aluminum implosion at stagnation ($t=120$ ns). The density spike on axis is due to stagnation of interior regions of the plasma that occurs before stagnation of the bulk plasma. These results are obtained from a one-dimensional calculation that was set up in accord with Sec. II and Ref. [13]. In this calculation only 0.1% of the mass was initially located in the region between the axis and 0.65 cm. Therefore most of the mass making up the hot core region, which extends out to 0.1 cm and represents 9% of the total mass of the plasma, comes from the interior edge of the bulk plasma. The majority of the 14.5 kJ/cm of K-shell photons produced in this calculation were generated in the denser plasma located just exterior to the hot core. Note that ion temperatures T_i are much greater than the electron temperatures T_e in Fig. 16 because ion heating of the electrons is slow compared to the rapid ion heating from thermalization of kinetic energy.

In one-dimensional magnetohydrodynamic calculations, inner mass is often present for calculational stability reasons. In an actual wire array implosion, arrays do not start as complete annular shells like gas puffs. Wires vaporize in a finite time with the outer part of the wire blowing up first. Plasma created in this manner would be magnetically pushed towards the axis in advance of plasma generated from the core of the wire.

Aivazov *et al.* [14] and Zakharov *et al.* [15] have observed plasmas streaming from the initial wire position to the pinch axis. These streams prefill the axis of the pinch with hot plasma that may also carry current. When the bulk of the mass arrives on axis, plasma already on axis will be shock heated. The prefilled plasma may also limit the compression (as has been observed with gas puffs [16]), thus reducing the density and hence radiated power. Certainly, for the extreme case of very thick wires, it has been observed that a core can be left at the original wire position as evidenced by shadows in time-integrated pinhole images [17].

The hypothesis that outer material from wire arrays preferentially gets into the axis (where it is heated) fits the data presented in this paper. Further substantiation of this hypothesis was found when, on one shot, we observed a 10-ns difference between the initial presence of magnesium K-shell x rays and aluminum K-shell x rays. This could only be due to the magnesium coating being

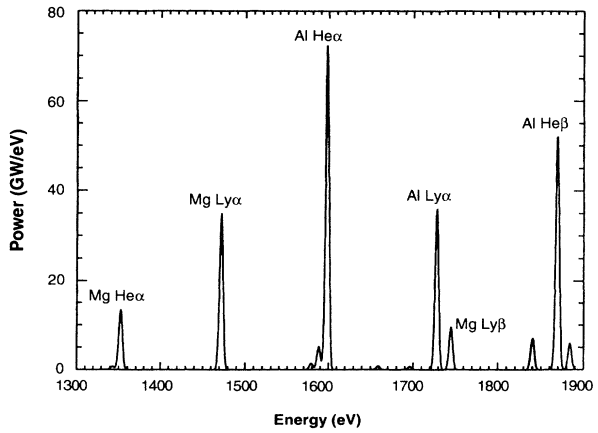

FIG. 14. Using a multizone CRE model with different temperatures and densities (see Table III), we can match the He-α and Ly-α lines.

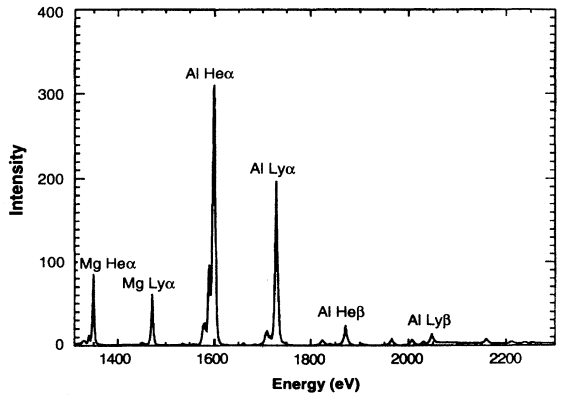

FIG. 15. Al-Mg alloy data from BJ5 (shot 3738) show a more consistant temperature (300–350 eV) between Al and Mg, indicating a uniform mix, as one would expect with an alloy.

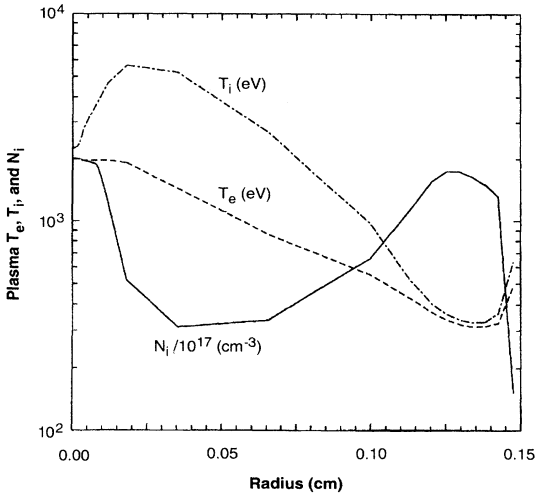

FIG. 16. Spatially resolved electron temperatures T_e, ion temperatures T_i, and ion densities N_i from a 300-μg/cm aluminum calculation at the stagnation time of 120 ns.

blown in ahead of the aluminum core material. It may also imply an increasing pinch temperature versus time. We need improved time resolution and timing of the MCP-gated crystal spectrometer to see if there is a consistent time difference between the onset of aluminum and magnesium K-shell x rays and to time resolve the complete implosion dynamics and possible temporal heating effects.

V. SUMMARY AND FUTURE WORK

In summary, our coated wire array experiments have experimentally demonstrated that the kilovolt x-ray radiation efficiencies of optically thick plasmas can be increased by mixing near-Z elements. Moreover, the magnesium-coated wire arrays have also allowed us to investigate some of the wire array dynamics. These results support the idea that the wires are not imploding as a shell, but rather the outer wire material is blown in ahead of the center of the wires. This precursor plasma achieved a higher temperature in the core and radiates very efficiently. If, as in the case discussed in this paper, the core plasma is a different element than the bulk plasma, then core radiation can escape the shell, contributing to enhanced yields.

Obviously, these results have significant impacts on wire array load design. As loads are scaled to higher current generators where higher masses will in turn cause higher-Z elements to become optically thick, mixing near-Z elements will allow experimenters to increase radiation efficiencies. Moreover, if the core plasma is hot and relatively dense, then coating a higher atomic number on the outside of the initial wires could be more useful (e.g., Al-Si loads). We are planning future experiments to study Al-Si loads, to better diagnose these pinches with time-resolved diagnostics, and to investigate the behavior of the coated loads as functions of wire number and initial diameter.

ACKNOWLEDGMENTS

We would like to thank Leonard Pressley, Pat Hebert, and Jed Rowley for their support and encouragement. The technical assistance of Ed Graper, Norm Knobel, Peter Laurence, and the Double-EAGLE crew is most appreciated. This work was supported by the Defense Nuclear Agency.

[1] C. Stallings, K. Nielsen, and R. Schneider, Appl. Phys. Lett. **29**, 404 (1976).
[2] C. Deeney, T. Nash, P. D. LePell, K. Childers, M. Krishnan, K. G. Whitney, and J. W. Thornhill, J. Quant. Spectrosc. Radiat. Transfer **44**, 457 (1990).
[3] C. Deeney, T. Nash, R. R. Prasad, L. Warren, K. G. Whitney, J. W. Thornhill, and M. C. Coulter, Phys. Rev. A **44**, 6762 (1991).
[4] M. Gersten, W. Clark, J. E. Rauch, G. M. Wilkinson, J. Katzenstein, R. D. Richardson, J. Davis, D. Duston, J. P. Apruzese, and R. Clark, Phys. Rev. A **33**, 477 (1986).
[5] K. G. Whitney, J. W. Thornhill, J. P. Apruzese, and J. Davis, J. Appl. Phys. **67**, 1725 (1990).
[6] J. P. Apruzese and J. Davis, J. Appl. Phys. **57**, 4349 (1985).
[7] M. C. Coulter, K. G. Whitney, and J. W. Thornhill, J. Quant. Spectrosc. Radiat. Transfer **44**, 443 (1990).
[8] P. Sincerny, D. Strachan, G. Frazier, C. Gilman, H. Halava, S. Wong, J. Banister, T. DaSilva, S. K. Lam, P. D. LePell, J. Levine, R. Rodenberg, and T. Sheridan (unpublished).
[9] T. Nash, C. Deeney, M. Krishna, R. R. Prasad, P. D. LePell, and L. Warren, J. Quant. Spectrosc. Radiat. Transfer **44**, 485 (1990).
[10] J. Katzenstein, J. Appl. Phys. **52**, 767 (1981).
[11] J. Giuliani, J. E. Rogerson, C. Deeney, T. Nash, R. R. Prasad, and M. Krishnan, J. Quant. Spectrosc. Radiat. Transfer **44**, 471 (1990).
[12] J. P. Apruzese, R. W. Clark, and J. W. Thornhill, J. Comput. Phys. (to be published).
[13] J. W. Thornhill, K. G. Whitney, C. Deeney, and P. D. LePell, Phys. Plasmas **1**, 321 (1994).
[14] I. K. Aivazov, V. D. Vikharev, G. S. Volkov, L. B. Nikandrov, V. P. Smirnov, and V. Ya. Tsarfin, Fiz. Plazmy **14**, 197 (1988) [Sov. J. Plasma Phys. **14**, 110 (1988)].
[15] S. M. Zakharov, G. V. Ivaanenkov, A. A. Kolomenskii, S. A. Pikuz, and A. I. Samokhin, Phys. Plazmy **13**, 201 (1987) [Sov. J. Plasma Phys. **13**, 115 (1987)].
[16] C. Deeney, P. D. LePell, F. L. Cochran, M. C. Coulter, K. G. Whitney, and J. Davis, Phys. Fluids B **5**, 992 (1993).
[17] J. C. Riordan, J. S. Pearlman, M. Gersten, and J. E. Rauch, in *Low-Energy X-Ray Diagnostics*, edited by David T. Attwood and Burton L. Henke, AIP Conf. Proc. No. 75 (AIP, New York, 1981), p. 35.

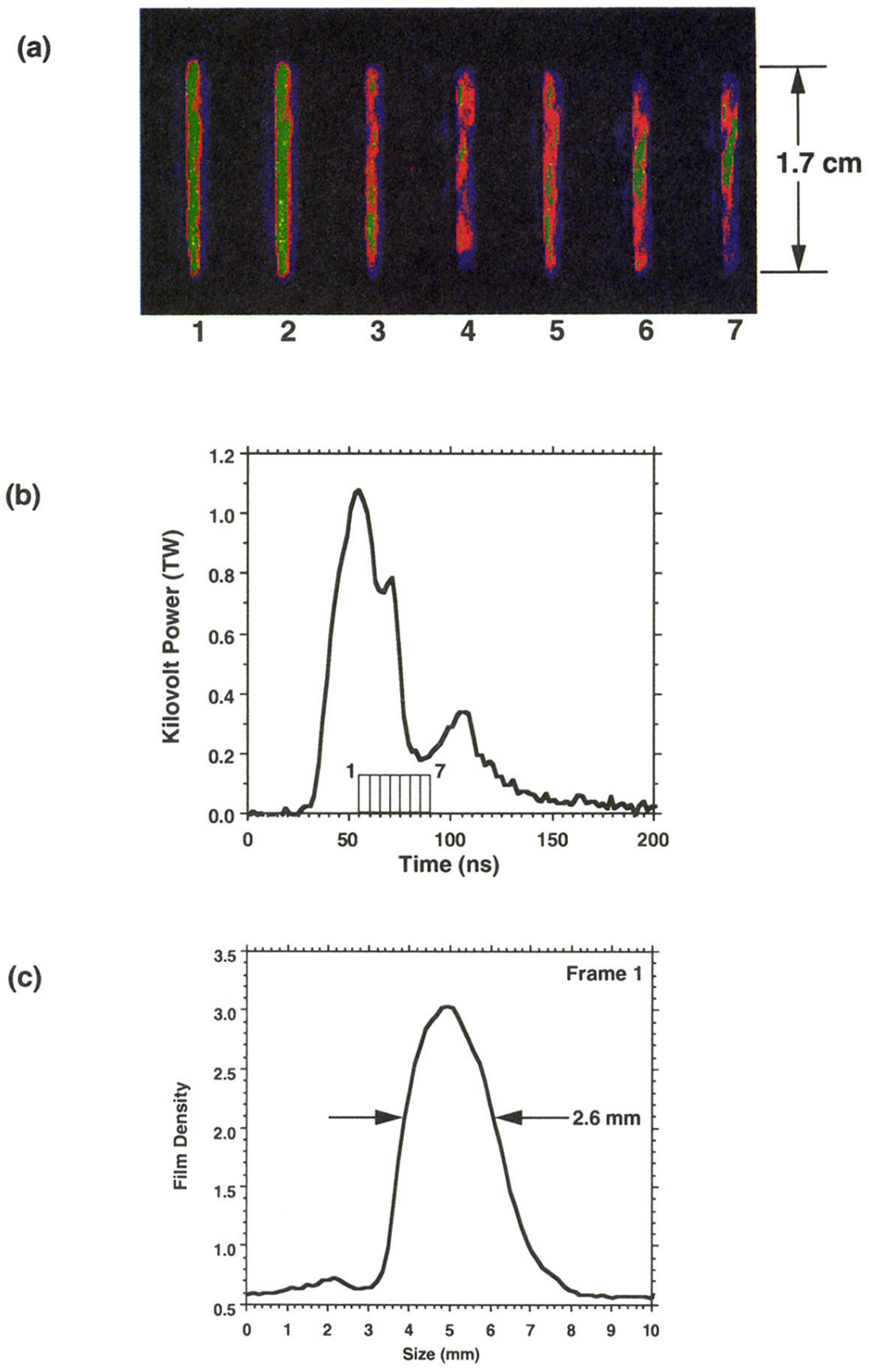

FIG. 11. Kilovolt time-resolved x-ray images of an 80%:20% implosion (shot 2814). In (a) we show the actual images in false color. The relationship of these images to the kilovolt power pulse are shown in (b) and an axially integrated, radial line out is shown in (c). Note that only a 1.7 cm length is observed due to the 22° viewing angle and the hardware geometry.